

# MAGNETIC ENERGY OF THE INTERGALACTIC MEDIUM FROM GALACTIC BLACK HOLES

P. P. KRONBERG,<sup>1</sup> Q. W. DUFTON,<sup>1</sup> H. LI,<sup>2</sup> AND S. A. COLGATE<sup>3</sup>

*Received 2001 March 27; accepted 2001 June 18*

## ABSTRACT

We present a quantitative analysis of two radio source samples having opposite extremes of ambient gas density that leads to important new conclusions about the magnetic energy in the intergalactic medium (IGM). We analyze here (1) a new, large sample of well-imaged “giant” extragalactic radio sources that are found in rarefied IGM environments and (2) at the other extreme, radio galaxies situated in the densest known IGM environments, within 150 kpc of rich cluster cores. We find that sources in the former sample contain magnetic energies  $E_B \sim 10^{60}$ – $10^{61}$  ergs and could be viewed as important “calorimeters” of the *minimum* energy a black hole (BH) accretion disk system injects into the IGM. In contrast to the radiation energy released by BH accretion, most of the magnetic energy is “trapped” initially in a volume, up to  $\sim 10^{73}$  cm<sup>3</sup>, around the host galaxy. But since these large, megaparsec-scale radio lobes are still overpressured after the active galactic nucleus phase (AGN), their subsequent expansion and diffusion will magnetize a large fraction of the entire IGM. This suggests that the energy stored in intergalactic magnetic fields will have a major, as yet underestimated effect on the evolution of subsequently forming galaxies. Comparison with the second, cluster core-embedded sample shows that the minimum magnetic energy  $E_B$  can be a strongly variable fraction of the inferred accretion energy  $E_{\text{acc}}$ , and that it depends on the ambient IGM environment. Cluster embedded AGNs inject significant energy as  $PdV$  work on the thermal ICM gas, and their magnetic energy, even ignoring the contribution from stellar and starburst outflows, is sufficient to account for that recently found beyond the inner cores of galaxy clusters. We discuss the various energy loss processes as these magnetized CR clouds (lobes) undergo their enormous expansion into the IGM. We conclude that the aggregate IGM magnetic energy derived purely from galactic black holes since the first epoch of significant galaxy BH formation is sufficiently large that it will have an important influence on the process of both galaxy and visible structure formation on scales up to  $\sim 1$  Mpc.

*Subject headings:* black hole physics — intergalactic medium — magnetic fields — radio continuum: galaxies

*On-line material:* machine-readable tables

## 1. INTRODUCTION

Advances in observational techniques have revealed the widespread existence of magnetic fields in the universe (see Kronberg 1994 for a review). Important questions at this point are how strong are the magnetic fields as derived from current observations, how widely are they distributed, where are they seeded, where and how are they amplified, and how much do they contribute to the energy budget of the intergalactic medium? It was pointed out over 30 years ago (Burbidge 1956; 1958) that a single galaxy releases a very large magnetic energy—up to  $\sim 10^{61}$  ergs—and that gravitational energy is the only feasible source (Hoyle et al. 1964; Burbidge & Burbidge 1965).

An excellent review by Begelman, Blandford, & Rees (1984) made a strong case for accretion on the central supermassive black holes as the energy engine for the powerful radio sources. Further progress has been made toward answering some of these questions (e.g., Bridle & Perley 1984; Wan, Daly, & Guerra 2000), and this paper presents a new analysis which focuses on AGN-fed, extended radio sources and their immediate intergalactic environment. The

analysis supports recent arguments (Colgate & Li 1999; 2000; Colgate, Li, & Pariev 2001) that a strong feedback effect might exist on the dynamics of the intergalactic medium (IGM) from the formation of supermassive black holes. A significant fraction of the energy released during these formation events could have been directly converted into magnetic field energy and magnetic flux, which are injected into extragalactic space.

The fact that extragalactic radio sources are seen in synchrotron radiation enables an approximate calculation of the minimum energy contained in the sources’ magnetic fields and relativistic particles. The jet-lobe morphology and commonly high polarization degree confirm, respectively, that the energizing source is at the host galaxy/quasar nucleus, and that the largest field ordering scales are comparable to, or greater than a galactic dimension. This latter fact sets constraints on the magnetic field generation process.

Recent Faraday rotation measurements (RM), in combination with X-ray bremsstrahlung data, have provided complementary probes of the strength and structure of magnetic fields *outside* of radio sources, but within the wider ambient hot *thermal* gas in galaxy clusters (see Kim et al. 1989, 1990; Taylor & Perley 1993; Feretti et al. 1995; Eilek 1999; Clarke, Kronberg, & Böhringer 2001). These studies, which used polarized synchrotron-emitting sources inside and/or behind clusters, have shown (Taylor & Perley 1993) that the central density-enhanced “cooling flow” regions ( $r \leq 150$  kpc) have magnetic fields up to  $\sim 40$   $\mu$ G,

<sup>1</sup> Department of Physics, University of Toronto, 60 St. George Street, Toronto M5S 1A7, Canada; kronberg@physics.utoronto.ca, dufton@physics.utoronto.ca.

<sup>2</sup> Applied Physics Division, MS B288, Los Alamos National Laboratory, Los Alamos, NM 87545; hli@lanl.gov.

<sup>3</sup> Theoretical Astrophysics, T-6, MS B288, Los Alamos National Laboratory, Los Alamos, NM 87545; colgate@lanl.gov.

with coherence scales up to  $\sim 50$  kpc. The most recent and definitive RM–X-ray probe of the wider cluster ICM ( $r \leq 1$  Mpc) beyond any cooling flow zones by Clarke et al. (2001) used a combination of background and cluster-internal radio sources to show that much of a rich galaxy cluster’s volume out to  $r = 500$  kpc is magnetized to a level of  $5 \mu\text{G}$  or more, implying a total cluster ICM magnetic energy of  $E_B \simeq 1.5 \times 10^{61} (r/500 \text{ kpc})^3 (B/5 \mu\text{G})^2 h_{75}^{-2}$  ergs. Given that cooling flows, to the extent they occur, are a later phenomenon of a cluster’s history, this result shows that galaxy clusters have been significantly, and previously, magnetized by processes other than cooling flows. We will offer an explanation for this important new result.

The important role of magnetic fields in clusters is also clearly demonstrated by the interaction between radio galaxies and their surrounding ICM, as revealed by recent Chandra observations. Large cavities in the X-ray-emitting gas correspond strikingly with the radio-bright lobes of the radio galaxies in Hydra A (McNamara et al. 2000) and in the Perseus cluster (Fabian et al. 2000). In both cases, an energy of at least  $\sim 10^{59}$  ergs is needed in order to displace the X-ray gas via  $PdV$  work. This energy is presumably supplied by the expanding magnetized radio lobes, and hence originated in the galaxy’s nucleus.

In this paper, we have analyzed  $\sim 100$  powerful extragalactic radio galaxies. We use them as indicators of the minimum net amount of magnetic energy, hence total energy that comes from a galactic black hole/accretion disk system. Since extended extragalactic radio sources really form a continuous distribution in many ways, we have chosen two categories with contrasting extremes of *external* ambient IGM pressure. These are the following:

1. Sources with large projected linear size,  $\geq 670 h_{75}^{-1}$  75 environment. They are referred to as “giant” sources, and we have compiled here a substantial list of  $\sim 70$  such sources, largely from the Northern Hemisphere, that are currently known and well imaged.
2.  $\sim 30$  sources located in the *densest* known IGM environments—within  $\sim 150$  kpc of the cores of rich clusters. We refer to them as “cluster sources” in this paper.

We argue that these giant sources can be used as “calorimeters” for the *minimum* amount of magnetic energy that galactic black holes have injected into intergalactic space since the cosmological epoch at which galactic black holes began to form.

We will conclude by showing that energies and magnetic flux injected into intergalactic space support recent work by Colgate & Li (1999, 2000) and Colgate et al. (2001), who proposed a mechanism for extracting the very large accretion energy of the commonly occurring  $\sim 10^8 M_\odot$  galactic black holes and releasing it directly into large intergalactic volumes. We briefly discuss some of the implications for galaxy formation, the physics of the IGM and cosmic magnetic fields.

## 2. MAGNETIC ENERGY IN RADIO GALAXIES

### 2.1. Data Compilation

In Table 1 we compile approximate estimates of the minimum total energy  $E_{\min}^{\text{tot}}$  (magnetic fields plus relativistic particles) and the minimum magnetic field  $B_{\min E}$  for a sample of well-imaged extragalactic radio sources from the

recent literature that have a projected largest linear size (LLS, from lobe to lobe) of  $\sim 0.67 h_{75}^{-1}$  Mpc or greater. The source volumes were estimated assuming a cylindrical source shape, where the length and radius of the cylinder are estimated based on the projected dimension as measured from the lowest reasonable contours from the radio images. We used the angular size distances,  $D_A = D_L / (1 + z)^2$ ,  $D_L$  being the luminosity distance.

These giant radio sources were primarily identified from three recent compilations of source data and images: Nilsson (1997), Ishwara-Chandra & Saikia (1999), and Schoenmakers et al. (2000b). Some additional sources in Table 1 are taken from other papers if they qualified as giants on our criterion. Spectral indices, flux densities, and other observable parameters were either obtained from the above primary sources or from other articles identified in the table. The images used to derive the numbers in Table 1 were at frequencies between 0.15 and 5 GHz, and where possible we also intercompared radio images at lower and higher frequencies within this range. In all such cases the results were found not to be significantly dependent on the frequency of the radio image used to calculate  $E_{\min}^{\text{tot}}$ . The *minimum* total energy  $E_{\min}^{\text{tot}}$  within a synchrotron-emitting volume ( $V$ ) containing relativistic particles and magnetic field can be expressed in terms of the measurables, luminosity, and volume

$$E_{\min}^{\text{tot}} = \left( \frac{3}{4\pi} \right)^{3/7} \mathcal{C}^{4/7} (1+k)^{4/7} (\phi V)^{3/7} L^{4/7} \text{ ergs}, \quad (1)$$

where we have approximately followed Pacholczyk (1970). Here  $k$  is the relativistic proton to electron energy ratio;  $\phi$  is the volume filling factor of the synchrotron emission;  $L$  is the integrated radio luminosity, calculated between fixed frequencies  $(\nu_1, \nu_2) = (10^7, 10^{10} \text{ Hz})$  in the emitted frame and  $z$ -corrected to the emitted frame; and  $\mathcal{C}$  is a slowly varying function of  $\alpha, \nu_1, \nu_2$ , where  $\alpha$  is defined by  $S \propto \nu^\alpha$ , and  $S$  is source’s spectral flux density. Because the radiating volumes reveal a characteristic filamentary structure, we conservatively adopted a global effective filling factor  $\phi = 0.1$ . Note that the total and magnetic energies are only mildly sensitive to  $\phi$ . The total energy is minimized when the magnetic field associated with the synchrotron radiation has the value

$$B_{\min E} = (6\pi)^{2/7} (1+k)^{2/7} \mathcal{C}^{2/7} (\phi V)^{-2/7} L^{2/7} \text{ G}, \quad (2)$$

again following the terminology of Pacholczyk (1970). Our calculations of  $E_{\min}^{\text{tot}}$  and  $B_{\min E}$  assume  $k = 100$ , which is close to the measured value for Galactic cosmic rays. The estimated  $E_{\min}^{\text{tot}}$  and  $B_{\min E}$  will be reduced by a factor of  $\sim 14$  and  $\sim 4$ , respectively, if  $k = 0$  is used. Furthermore, using  $\phi = 1$  will increase  $E_{\min}^{\text{tot}}$  by a factor of 2.7 but decrease  $B_{\min E}$  by 2.

The integrated flux densities for each source were checked against standard compilations of flux densities to test if the image used contained a substantial fraction of the source’s entire synchrotron luminosity. Where substantial differences were noted alternative images were selected. The source volume estimates (col. [6] of Table 1) were based on the most sensitive available image, and  $H_0 = 75$ ,  $\Omega = 1$ . The volume, hence total energy and magnetic field estimates in Table 1 must be interpreted as only global, approximate estimates for any given source, since an optimally precise calculation of  $E_{\min}^{\text{tot}}$  and  $B_{\min E}$  would require a detailed inte-

gration over an assumed three-dimensional emissivity distribution. This is not possible to do in a consistent way at present, given the inhomogeneity of the currently available sample. Our global estimate of the uncertainties are  $\sim \pm 30\%$  for  $E_{\min}^{\text{tot}}$ . Such errors do not include systematics such as (1) the unknown projection angle of a given source into the plane of the sky, or (2) any undetected “halo flux”—both of which could systematically increase our estimates of  $E_{\min}^{\text{tot}}$  by an unknown but potentially large amount (e.g., the extended halo around M87).

Table 2 lists the same measured and calculated quantities as in Table 1, but is restricted to extended radio galaxies that are located within 150 kpc (projected) of the cores of rich galaxy clusters (see Table 2 for references). These

cluster sources include some very well-studied sources, for some of which there are not only detailed images of the synchrotron radio emission, but also of Faraday rotation and detailed recent X-ray images from the *ROSAT* and/or *Chandra* satellites. Such cases allow both the sources and their cluster environments to be independently probed; That is, we can compare the energy in the synchrotron-emitting cosmic-ray gas magnetic fields with that of the ambient thermal ICM. Where possible, the cluster source morphologies were compared in detail with recent X-ray images. The latter show a striking effect, namely, that the bremsstrahlung-emitting ambient intracluster gas gets displaced by the cosmic-ray gas of the radio lobes. Recent examples are the depressions in the (projected) X-ray

TABLE 1  
GIANT RADIO SOURCE PROPERTIES

Source (1)	Name (2)	$z$ (3)	$\alpha$ (4)	Luminosity ( $\text{ergs s}^{-1}$ ) (5)	Volume ( $\text{cm}^3$ ) (6)	$E_{\min}^{\text{tot}}$ ( $\text{ergs}$ ) (7)	$B_{\min}^{\text{tot}}$ (Gauss) (8)	References (9)
0017–205 .....	MRC	0.197	–0.78	$4.85 \times 10^{42}$	$5.02 \times 10^{71}$	$8.34 \times 10^{59}$	$1.37 \times 10^{-5}$	1
0050+402 .....	...	0.1488	–0.82	$1.56 \times 10^{42}$	$1.45 \times 10^{72}$	$6.95 \times 10^{59}$	$7.35 \times 10^{-6}$	2, 3
0055+300 .....	NGC 315	0.0167	–0.59	$1.27 \times 10^{41}$	$2.68 \times 10^{72}$	$2.18 \times 10^{59}$	$3.03 \times 10^{-6}$	4, 5
0109+492 .....	3C 35	0.067	–0.86	$1.71 \times 10^{42}$	$8.59 \times 10^{71}$	$5.90 \times 10^{59}$	$8.81 \times 10^{-6}$	6
0114–476 .....	PKS	0.146	–0.47	$1.01 \times 10^{43}$	$6.07 \times 10^{72}$	$3.62 \times 10^{60}$	$8.22 \times 10^{-6}$	7
0132+376 .....	3C 46	0.4373	–1.03	$4.87 \times 10^{43}$	$2.46 \times 10^{71}$	$2.36 \times 10^{60}$	$3.30 \times 10^{-5}$	8
0136+397 .....	4C 39.04	0.2107	–0.87	$6.59 \times 10^{42}$	$1.02 \times 10^{72}$	$1.36 \times 10^{60}$	$1.23 \times 10^{-5}$	8, 9
0157+405 .....	4C 40.08	0.078	–0.92	$1.33 \times 10^{42}$	$4.06 \times 10^{72}$	$9.98 \times 10^{59}$	$5.27 \times 10^{-6}$	10
0211+326 .....	...	0.2605	–0.84	$5.92 \times 10^{42}$	$3.78 \times 10^{72}$	$2.23 \times 10^{60}$	$8.16 \times 10^{-6}$	2, 3
0211–479 .....	PKS	0.2195	–0.83	$1.04 \times 10^{43}$	$8.22 \times 10^{71}$	$1.60 \times 10^{60}$	$1.48 \times 10^{-5}$	7
0309+411 .....	B3	0.136	–0.8	$1.41 \times 10^{42}$	$8.46 \times 10^{72}$	$1.39 \times 10^{60}$	$4.32 \times 10^{-6}$	11
0313+683 .....	WENSS	0.0902	–0.95	$1.22 \times 10^{42}$	$2.86 \times 10^{72}$	$8.15 \times 10^{59}$	$5.68 \times 10^{-6}$	12
0313–271 .....	MRC	0.216	–1.14	$4.99 \times 10^{42}$	$7.72 \times 10^{71}$	$1.06 \times 10^{60}$	$1.25 \times 10^{-5}$	1
0319–454 .....	PKS	0.0633	–0.75	$2.40 \times 10^{42}$	$5.05 \times 10^{72}$	$1.52 \times 10^{60}$	$5.84 \times 10^{-6}$	13, 14
0424–728 .....	PKS	0.1921	–1.05	$7.79 \times 10^{42}$	$1.13 \times 10^{72}$	$1.59 \times 10^{60}$	$1.26 \times 10^{-5}$	7
0437–244 .....	MRC	0.84	–0.94	$7.61 \times 10^{43}$	$1.81 \times 10^{71}$	$2.61 \times 10^{60}$	$4.03 \times 10^{-5}$	...
0448+519 .....	3C 130	0.109	–0.85	$5.60 \times 10^{42}$	$8.93 \times 10^{71}$	$1.18 \times 10^{60}$	$1.22 \times 10^{-5}$	4
0503–286 .....	MRC	0.038	–1.1	$7.35 \times 10^{41}$	$1.97 \times 10^{72}$	$5.23 \times 10^{59}$	$5.48 \times 10^{-6}$	15, 16
0511–305 .....	PMN	0.0583	–0.84	$1.73 \times 10^{42}$	$4.72 \times 10^{71}$	$4.59 \times 10^{59}$	$1.05 \times 10^{-5}$	7
0634–205 .....	PMN	0.056	–0.87	$4.13 \times 10^{42}$	$3.31 \times 10^{71}$	$6.50 \times 10^{59}$	$1.49 \times 10^{-5}$	17, 18
0648+733 .....	...	0.1145	–0.66	$1.84 \times 10^{42}$	$1.93 \times 10^{72}$	$8.55 \times 10^{59}$	$7.08 \times 10^{-6}$	2, 3
0654+482 .....	7C	0.776	–0.75	$1.33 \times 10^{43}$	$3.31 \times 10^{72}$	$3.14 \times 10^{60}$	$1.04 \times 10^{-5}$	3, 19
0658+490 .....	...	0.065	–0.64	$2.60 \times 10^{41}$	$6.04 \times 10^{71}$	$1.71 \times 10^{59}$	$5.66 \times 10^{-6}$	2, 3
0707–359 .....	PKS	0.2182	–0.72	$1.56 \times 10^{43}$	$2.19 \times 10^{72}$	$3.04 \times 10^{60}$	$1.25 \times 10^{-5}$	7
0744+558 .....	DA 240	0.0356	–0.89	$1.13 \times 10^{42}$	$6.45 \times 10^{72}$	$1.11 \times 10^{60}$	$4.41 \times 10^{-6}$	5, 20
0813+758 .....	...	0.2324	–0.74	$6.57 \times 10^{42}$	$6.39 \times 10^{72}$	$2.93 \times 10^{60}$	$7.20 \times 10^{-6}$	2, 3
0821+695 .....	8C	0.538	–1.14	$9.51 \times 10^{42}$	$2.38 \times 10^{72}$	$2.53 \times 10^{60}$	$1.10 \times 10^{-5}$	21, 22
0915+320 .....	B2	0.062	–0.5	$1.64 \times 10^{41}$	$1.08 \times 10^{71}$	$6.29 \times 10^{58}$	$8.10 \times 10^{-6}$	23
0945+734 .....	4C 73.08	0.0581	–0.85	$1.44 \times 10^{42}$	$1.58 \times 10^{72}$	$6.94 \times 10^{59}$	$7.05 \times 10^{-6}$	24
1003+351 .....	3C 236	0.0988	–0.61	$7.25 \times 10^{42}$	$1.01 \times 10^{73}$	$3.81 \times 10^{60}$	$6.53 \times 10^{-6}$	5
1025–229 .....	MRC	0.309	–0.9	$9.95 \times 10^{42}$	$2.00 \times 10^{71}$	$8.54 \times 10^{59}$	$2.20 \times 10^{-5}$	...
1029+571 .....	HB 13	0.034	–0.85	$1.13 \times 10^{41}$	$6.91 \times 10^{70}$	$4.25 \times 10^{58}$	$8.34 \times 10^{-6}$	4, 25
1058+368 .....	7C	0.75	–0.75	$1.98 \times 10^{43}$	$3.24 \times 10^{72}$	$3.92 \times 10^{60}$	$1.17 \times 10^{-5}$	3, 19
1127–130 .....	PKS	0.6337	–0.87	$7.28 \times 10^{43}$	$1.60 \times 10^{71}$	$2.37 \times 10^{60}$	$4.10 \times 10^{-5}$	26
1144+352 .....	WENSS	0.063	–0.56	$3.78 \times 10^{40}$	$2.10 \times 10^{71}$	$3.61 \times 10^{58}$	$4.42 \times 10^{-6}$	27, 28
1158+351 .....	87GB	0.55	–1.1	$1.90 \times 10^{43}$	$4.99 \times 10^{71}$	$1.91 \times 10^{60}$	$2.08 \times 10^{-5}$	29
1209+745 .....	4C 74.17	0.107	–0.85	$1.13 \times 10^{42}$	$4.77 \times 10^{71}$	$3.60 \times 10^{59}$	$9.24 \times 10^{-6}$	30
1213+422 .....	...	0.2426	–0.83	$3.66 \times 10^{42}$	$4.06 \times 10^{72}$	$1.74 \times 10^{60}$	$6.97 \times 10^{-6}$	2, 3
1218+639 .....	TXS	0.2	–0.85	$2.62 \times 10^{42}$	$3.11 \times 10^{72}$	$1.29 \times 10^{60}$	$6.86 \times 10^{-6}$	31
1232+216 .....	3C 274.1	0.422	–0.92	$7.83 \times 10^{43}$	$4.32 \times 10^{71}$	$3.86 \times 10^{60}$	$3.18 \times 10^{-5}$	32
1309+412 .....	...	0.1103	–0.83	$9.51 \times 10^{41}$	$3.66 \times 10^{71}$	$2.91 \times 10^{59}$	$9.49 \times 10^{-6}$	2, 10
1312+698 .....	DA 340	0.106	–0.73	$2.48 \times 10^{42}$	$5.56 \times 10^{71}$	$5.99 \times 10^{59}$	$1.10 \times 10^{-5}$	2, 31
1331–099 .....	PKS	0.081	–0.9	$2.47 \times 10^{42}$	$1.42 \times 10^{72}$	$9.04 \times 10^{59}$	$8.48 \times 10^{-6}$	3, 33
1349+647 .....	3C 292	0.71	–0.8	$2.08 \times 10^{44}$	$9.13 \times 10^{70}$	$3.32 \times 10^{60}$	$6.41 \times 10^{-5}$	34, 35
1358+305 .....	B2	0.206	–0.99	$3.77 \times 10^{42}$	$5.83 \times 10^{72}$	$2.11 \times 10^{60}$	$6.40 \times 10^{-6}$	36
1426+295 .....	...	0.087	–0.78	$4.34 \times 10^{41}$	$1.40 \times 10^{72}$	$3.30 \times 10^{59}$	$5.17 \times 10^{-6}$	2, 3
1450+333 .....	...	0.249	–0.94	$4.57 \times 10^{42}$	$3.79 \times 10^{72}$	$1.95 \times 10^{60}$	$7.63 \times 10^{-6}$	2, 3
1452–517 .....	MRC	0.08	–0.3	$3.45 \times 10^{42}$	$4.03 \times 10^{72}$	$1.66 \times 10^{60}$	$6.83 \times 10^{-6}$	37
1519+513 .....	87GB	0.37	–0.88	$3.29 \times 10^{43}$	$1.08 \times 10^{72}$	$3.48 \times 10^{60}$	$1.90 \times 10^{-5}$	29
1543+845 .....	...	0.201	–0.89	$2.26 \times 10^{42}$	$3.15 \times 10^{72}$	$1.20 \times 10^{60}$	$6.56 \times 10^{-6}$	2, 3
1545–321 .....	PKS	0.1085	–0.94	$3.43 \times 10^{42}$	$4.71 \times 10^{71}$	$6.80 \times 10^{59}$	$1.28 \times 10^{-5}$	7

TABLE 1—*Continued*

Source (1)	Name (2)	$z$ (3)	$\alpha$ (4)	Luminosity (ergs s <sup>-1</sup> ) (5)	Volume (cm <sup>3</sup> ) (6)	$E_{\min}(\text{tot})$ (ergs) (7)	$B_{\min}(\text{tot})$ (Gauss) (8)	References (9)
1549+202 .....	3C 326	0.0895	-0.82	$4.79 \times 10^{42}$	$5.02 \times 10^{72}$	$2.26 \times 10^{60}$	$7.13 \times 10^{-6}$	5, 38
1602+376 .....	7C	0.814	-0.75	$2.28 \times 10^{43}$	$5.83 \times 10^{72}$	$5.43 \times 10^{60}$	$1.03 \times 10^{-5}$	3, 19
1626+518 .....	WENSS	0.056	-0.66	$3.31 \times 10^{41}$	$4.14 \times 10^{71}$	$1.68 \times 10^{59}$	$6.77 \times 10^{-6}$	2, 39
1636+418 .....	7C	0.867	-0.75	$1.24 \times 10^{43}$	$2.76 \times 10^{72}$	$2.77 \times 10^{60}$	$1.07 \times 10^{-5}$	3, 19
1637+826 .....	NGC 6251	0.023	-0.58	$3.68 \times 10^{41}$	$2.94 \times 10^{72}$	$4.15 \times 10^{59}$	$4.00 \times 10^{-6}$	5, 40
1701+423 .....	7C	0.476	-0.75	$8.89 \times 10^{42}$	$3.60 \times 10^{72}$	$2.66 \times 10^{60}$	$9.13 \times 10^{-6}$	3, 19
1721+343 .....	4C 34.47	0.2055	-0.75	$9.44 \times 10^{42}$	$5.28 \times 10^{71}$	$1.24 \times 10^{60}$	$1.63 \times 10^{-5}$	41
1834+620 .....	WENSS	0.519	-0.97	$4.23 \times 10^{43}$	$2.14 \times 10^{71}$	$2.03 \times 10^{60}$	$3.28 \times 10^{-5}$	42, 43
1910-800 .....	PKS	0.346	-0.91	$1.88 \times 10^{43}$	$1.08 \times 10^{72}$	$2.53 \times 10^{60}$	$1.63 \times 10^{-5}$	7
1918+516 .....	...	0.284	-0.91	$4.87 \times 10^{42}$	$5.49 \times 10^{72}$	$2.36 \times 10^{60}$	$6.97 \times 10^{-6}$	2, 3
2043+749 .....	4C 74.26	0.104	-0.81	$2.53 \times 10^{42}$	$1.89 \times 10^{72}$	$1.03 \times 10^{60}$	$7.84 \times 10^{-6}$	2, 44
2147+816 .....	...	0.1457	-0.45	$1.89 \times 10^{42}$	$5.75 \times 10^{72}$	$1.36 \times 10^{60}$	$5.17 \times 10^{-6}$	2, 45
2309+184 .....	3C 457	0.427	-1.02	$8.08 \times 10^{43}$	$4.74 \times 10^{71}$	$4.18 \times 10^{60}$	$3.16 \times 10^{-5}$	46

NOTE.—Table 1 is also available in machine-readable form in the electronic version of the *Astrophysical Journal*.

REFERENCES—(1) Kapahi et al. 1998; (2) Schoenmakers et al. 2000b; (3) Condon et al. 1998; (4) Jagers 1987b; (5) Mack et al. 1997; (6) Jagers 1987a; (7) Subrahmanyan, Saripalli, & Hunstead 1996; (8) Gregorini et al. 1988; (9) Hine 1979; (10) Vigotti et al. 1989; (11) de Bruyn 1989; (12) Schoenmakers et al. 1998; (13) Jones & McAdam 1992; (14) Saripalli et al. 1994; (15) Saripalli et al. 1986; (16) Subrahmanya & Hunstead 1986; (17) Kronberg, Wielebinski, & Graham 1986; (18) Danziger, Goss, & Frater 1978; (19) Cotter et al. 1996; (20) Strom, Baker, & Willis 1981; (21) Lacy et al. 1993; (22) Lara et al. 2000; (23) Ekers et al. 1981; (24) Mayer 1979; (25) Masson 1979; (26) Bhatnagar, Gopal-Krishna, & Wisotzki 1998; (27) Schoenmakers et al. 1999; (28) Snellen et al. 1995; (29) Machalski & Condon 1985; (30) van Breugel & Willis 1981; (31) Saunders, Baldwin, & Warner 1987; (32) Strom et al. 1990; (33) Saripalli et al. 1996; (34) Alexander & Leahy 1987; (35) Leahy, Pooley, & Riley 1986; (36) Parma et al. 1996; (37) Jones 1986; (38) Willis & Strom 1978; (39) Röttgering et al. 1996; (40) Willis et al. 1982; (41) Jägers et al. 1982; (42) Schoenmakers et al. 2000a; (43) Lara et al. 1999; (44) Riley et al. 1989; (45) Palma et al. 2000; (46) Leahy & Perley 1991.

surface brightness that clearly coincide with the periphery of radio lobes of Hydra A (McNamara et al. 2000) and the arcmin-scale lobes of Perseus A (3C 84) (Fabian et al. 2000). In addition, there have been a half dozen or so detections of X-rays from knots/jets (e.g., Wilson, Young, & Shopbell 2001), which sometimes allow an independent measure, or limit for the magnetic field strength. In general we find our equipartition field strength is roughly consistent with, or slightly lower than these estimates.

## 2.2. IGM Energy Supply from Radio Sources outside of Rich Clusters

It is widely believed that the energy contained in extended radio galaxies is supplied by the central supermassive black hole. The average estimated  $E_{\min}^{\text{tot}}$  for the “giant” sources reaches  $\sim 10^{61}$  ergs, which is a significant fraction of the gravitational energy released during the formation of supermassive black holes in the centers of these active galaxies (i.e.,  $\sim 10^{62}$  ergs for a  $10^8 M_{\odot}$  black hole).

### 2.2.1. $E_{\min}^{\text{tot}}$ as a Minimum Estimate for the Total Black Hole Energy

It is important to realize that the observed magnetic energy in radio sources will *understate* the true total magnetic energy released by the accretion onto black holes. Some additional energy will have been lost through various processes as magnetic fields are transported from near the black hole (size of  $\sim$  AU) to the lobes ( $\sim$  megaparsec). Further, after the energy has been deposited from the jet into the lobes, the relativistic particles will lose energy through radiative cooling by (1) inverse-Compton and (2) synchrotron radiation losses, as well as by possible (3) ionization losses and (4) particle escape. In addition, given the very large volumes of these sources, some unknown amount (5) of  $PdV$  work, and (6) whatever free expansion energy will have been expended by the time we observe the source. To these unquantified additions to the BH energy release, we must further augment the calculated minimum energies in

Tables 1 and 2 by an increase to  $V$  due to deprojection and also due to any faint undetected synchrotron halo volumes that the limited sensitivity of a radio map may not have revealed—as mentioned above.

In addition, as stated above, these minimum energies are presumed to be half magnetic, the remaining half being either 49.5% protons of any energy and 0.5% electrons of gamma =  $10^4$ – $10^5$  (10–100 GeV), or all electrons of this energy. These energetic particles are accelerated by an unknown mechanism, and it is important to note that the total energy in a giant radio source is  $\sim 10^7$  greater than the same CRs within our Galaxy. The efficiency of acceleration may be much less in many cases and thus the magnetic fields correspondingly larger.

Finally, our adopted  $\nu_2 = 10$  GHz; hence  $L$  (col. [5]) can be demonstrated to be conservatively low for some sources, which are known to radiate above 10 GHz. Thus any or all of the foregoing energy losses and systematic energy underestimates will not be represented in our  $E_{\min}^{\text{tot}}$  tabulated in column (7), so that these values will tend to understate the true total energy released by the AGN black hole/accretion disk. The important point is that they are firm lower limits. The giant radio sources, as we shall demonstrate below, have accumulated the largest amount of cosmic-ray and magnetic energy outside of the parent galaxy. We will argue that they are especially well suited as probes, or “calorimeters” of the accumulated black hole magnetic energy released into the IGM space over the source’s radiative lifetime. Because such sources last only a fraction,  $\leq 1\%$ , of a Hubble time, they are important fiducial systems for calculating the total magnetic energy of the mature universe.

The typical volume occupied by the lobes of a single galaxy in Table 1, is  $\sim 10^{72}$ – $10^{73}$  cm<sup>3</sup>, a fraction of Mpc<sup>3</sup>. Even at these large volumes, these lobes appear to be over-pressured compared to the surrounding medium. This is indicated by our estimates of the mean minimum magnetic

TABLE 2  
CLUSTER SOURCE PROPERTIES

Source (1)	Name (2)	$z$ (3)	$\alpha$ (4)	Luminosity ( $\text{ergs s}^{-1}$ ) (5)	Volume ( $\text{cm}^3$ ) (6)	$E_{\text{min}}(\text{tot})$ ( $\text{ergs}$ ) (7)	$B_{\text{min}}(\text{tot})$ (Gauss) (8)	References (9)
0019+230...	4C 23.01	0.1332	-1.12	$8.76 \times 10^{41}$	$2.69 \times 10^{69}$	$3.44 \times 10^{58}$	$3.81 \times 10^{-5}$	1
0037+209...	...	0.0579	-0.78	$7.32 \times 10^{40}$	$8.86 \times 10^{69}$	$1.37 \times 10^{58}$	$1.32 \times 10^{-5}$	1
0043+201...	4C 20.04	0.1063	-0.8	$1.62 \times 10^{42}$	$9.23 \times 10^{69}$	$8.15 \times 10^{58}$	$3.16 \times 10^{-5}$	2
0053-015...	...	0.03822	-1.01	$4.35 \times 10^{41}$	$5.55 \times 10^{69}$	$3.13 \times 10^{58}$	$2.52 \times 10^{-5}$	3, 4
0110+152...	...	0.0447	-0.85	$3.18 \times 10^{41}$	$7.35 \times 10^{69}$	$2.94 \times 10^{58}$	$2.13 \times 10^{-5}$	2
0124+189...	4C 18.06	0.04268	-0.48	$3.56 \times 10^{41}$	$2.68 \times 10^{68}$	$7.52 \times 10^{57}$	$5.63 \times 10^{-5}$	1
0154+320...	...	0.0891	-0.88	$4.96 \times 10^{41}$	$1.21 \times 10^{69}$	$1.74 \times 10^{58}$	$4.04 \times 10^{-5}$	1
0255+058...	3C 75	0.023153	-0.78	$4.57 \times 10^{41}$	$2.30 \times 10^{69}$	$2.20 \times 10^{58}$	$3.29 \times 10^{-5}$	5
0320-373...	Fornax A	0.00587	-0.55	$6.01 \times 10^{41}$	$1.58 \times 10^{71}$	$1.58 \times 10^{59}$	$1.06 \times 10^{-5}$	6
0719+670...	4C 67.13	0.08723	-0.7	$7.08 \times 10^{41}$	$9.02 \times 10^{68}$	$1.87 \times 10^{58}$	$4.84 \times 10^{-5}$	1
0756+272...	...	0.0991	-1.01	$9.53 \times 10^{41}$	$8.53 \times 10^{69}$	$5.88 \times 10^{58}$	$2.79 \times 10^{-5}$	1
0803-008...	3C 193	0.0891	-0.8	$1.63 \times 10^{42}$	$5.34 \times 10^{69}$	$6.46 \times 10^{58}$	$3.70 \times 10^{-5}$	1
0836+290...	4C 29.30	0.0788	-0.85	$8.08 \times 10^{41}$	$2.85 \times 10^{70}$	$8.91 \times 10^{58}$	$1.88 \times 10^{-5}$	2
0915-118...	Hydra A	0.053	-0.93	$2.20 \times 10^{43}$	$7.57 \times 10^{67}$	$4.65 \times 10^{58}$	$2.64 \times 10^{-4}$	7
1159+583...	4C 58.23	0.1018	-0.8	$1.65 \times 10^{42}$	$2.52 \times 10^{68}$	$1.76 \times 10^{58}$	$8.89 \times 10^{-5}$	2
1222+131...	3C 272.1	0.003429	-0.6	$1.03 \times 10^{40}$	$2.19 \times 10^{66}$	$1.28 \times 10^{56}$	$8.13 \times 10^{-5}$	8, 9
1231+674...	4C 67.12	0.1062	-0.9	$1.75 \times 10^{42}$	$1.75 \times 10^{69}$	$4.20 \times 10^{58}$	$5.21 \times 10^{-5}$	2
1233+169...	PKS	0.0784	-0.51	$5.78 \times 10^{41}$	$6.18 \times 10^{69}$	$3.77 \times 10^{58}$	$2.63 \times 10^{-5}$	1
1246-410...	NGC 4696	0.0099	-0.84	$6.06 \times 10^{40}$	$1.84 \times 10^{66}$	$3.26 \times 10^{56}$	$1.42 \times 10^{-4}$	10
1256+281...	5C4.81	0.0235	-1.13	$5.35 \times 10^{40}$	$1.05 \times 10^{69}$	$4.63 \times 10^{57}$	$2.23 \times 10^{-5}$	11
1409+52...	3C 295	0.461	-0.98	$1.08 \times 10^{45}$	$1.08 \times 10^{67}$	$1.87 \times 10^{59}$	$1.40 \times 10^{-3}$	12
1433+553...	4C 55.29	0.1396	-0.7	$1.52 \times 10^{42}$	$8.00 \times 10^{68}$	$2.72 \times 10^{58}$	$6.21 \times 10^{-5}$	2
1508+065...	...	0.08086	-0.83	$5.80 \times 10^{41}$	$1.96 \times 10^{68}$	$8.71 \times 10^{57}$	$7.10 \times 10^{-5}$	1
1638+558...	...	0.2426	-0.8	$2.75 \times 10^{42}$	$1.14 \times 10^{70}$	$1.19 \times 10^{59}$	$3.43 \times 10^{-5}$	1
1820+689...	4C 68.21	0.0881	-0.63	$9.25 \times 10^{41}$	$7.42 \times 10^{69}$	$5.35 \times 10^{58}$	$2.86 \times 10^{-5}$	1
1826+747...	...	0.121	-0.8	$1.41 \times 10^{42}$	$2.62 \times 10^{68}$	$1.63 \times 10^{58}$	$8.40 \times 10^{-5}$	2
1957+405...	Cygnus A	0.056075	-1.01	$9.14 \times 10^{44}$	$3.10 \times 10^{69}$	$1.93 \times 10^{60}$	$2.65 \times 10^{-4}$	13, 14, 15
2229-086...	PKS	0.0831	-0.52	$8.38 \times 10^{41}$	$2.51 \times 10^{70}$	$8.49 \times 10^{58}$	$1.96 \times 10^{-5}$	1
2236-176...	...	0.0698	-0.55	$1.22 \times 10^{42}$	$8.02 \times 10^{68}$	$2.41 \times 10^{58}$	$5.83 \times 10^{-5}$	2
2335+267...	3C 465	0.030221	-0.84	$1.10 \times 10^{42}$	$5.07 \times 10^{69}$	$5.10 \times 10^{58}$	$3.37 \times 10^{-5}$	16
3C 84.....	Perseus A (halo)	0.017559	-1.1	$3.28 \times 10^{41}$	$5.87 \times 10^{70}$	$7.31 \times 10^{58}$	$1.19 \times 10^{-5}$	17, 18
3C 84.....	Perseus A (inner arcmin)	0.017559	-1.01	$1.33 \times 10^{41}$	$3.84 \times 10^{67}$	$1.88 \times 10^{57}$	$7.44 \times 10^{-5}$	
3C 274.....	Virgo A (halo only)	0.00436	-1.1	$3.00 \times 10^{41}$	$1.90 \times 10^{69}$	$1.60 \times 10^{58}$	$3.08 \times 10^{-5}$	18, 19, 20, 21, 22, 23
3C 274.....	Virgo A (inner radio core)	0.00436	-0.5	$3.31 \times 10^{41}$	$5.28 \times 10^{65}$	$5.04 \times 10^{56}$	$3.29 \times 10^{-4}$	

NOTE.—Table 2 is also available in machine-readable form in the electronic version of the *Astrophysical Journal*.

REFERENCES—(1) Owen & Ledlow 1997; (2) O'Donoghue et al. 1990; (3) Feretti et al. 1999; (4) O'Dea & Owen 1985; (5) Owen et al. 1985; (6) Ekers et al. 1983; (7) Taylor et al. 1990; (8) Laing & Bridle 1987; (9) Zukowski 1990; (10) Taylor, Allen & Fabian 1999; (11) Dallacasa et al. 1989; (12) Perley & Taylor 1991; (13) Carilli et al. 1991; (14) Baars et al. 1977; (15) Hargrave & Ryle 1974; (16) Eilek et al. 1984; (17) Pedlar et al. 1990; (18) Herbig & Readhead 1992; (19) Kassim et al. 1993; (20) Andernach et al. 1979; (21) Rottmann et al. 1996; (22) Hines, Eilek, & Owen 1989; (23) Turland 1975.

field strengths,  $\sim 5 \mu\text{G}$ , corresponding to magnetic pressures  $\sim 10^{-12} \text{ dyn cm}^{-2}$  that are much higher than the typical thermal pressure of the IGM— $\sim 10^{-15} n_5 T_6 \text{ dyn cm}^{-2}$  for an assumed mean IGM density of  $10^{-5} \text{ cm}^{-3}$  and a temperature of  $10^6 \text{ K}$ . These giant radio lobes are therefore expected to expand further, occupying even larger volumes as they evolve. The details of this volume filling process are yet to be understood.

### 2.2.2. Magnetic Energy as “Captured” Energy Release from Galactic Black Holes

It follows from the above discussion that a substantial fraction of the energy stored in extended extragalactic radio sources is probably in the form of magnetic energy. This presents a quite different picture from other forms of energy release, such as the intense radiation from AGNs. Apart from ionizing the medium, the radiation energy quickly loses its dynamical impact when the surrounding medium becomes optically thin. For magnetic fields, however, most of its energy has been retained/confined within a large volume (large compared to its “engine” size but much

smaller than the volume that radiation would have filled) for a significant fraction of cosmic time. An important consequence of outward transported magnetic fields is that this energy remains *dynamically* important, perhaps for the age of the universe, thereby providing a *much stronger interaction with the surrounding matter* than the radiation will have.

### 2.3. Comparison of the Energy Content of “Giant” and “Cluster” Sources

Figure 1, in which we separate the “giant” and “cluster” sample, shows the interrelations between the quantities tabulated above. The plot of size LLS versus luminosity  $L$  in Figure 1a shows that the average radio luminosity for cluster radio sources is generally lower than that of the “giant” sources, although there is considerable overlap. Although the noncluster sources do not include those with  $LLS < 0.67 h_{75}^{-1} \text{ Mpc}$ , and are not complete to a fixed lower flux density or luminosity limit, they are consistent with well-established monochromatic radio power ( $P$ ) versus LLS plots, that also show little correlation of  $P$  with LLS

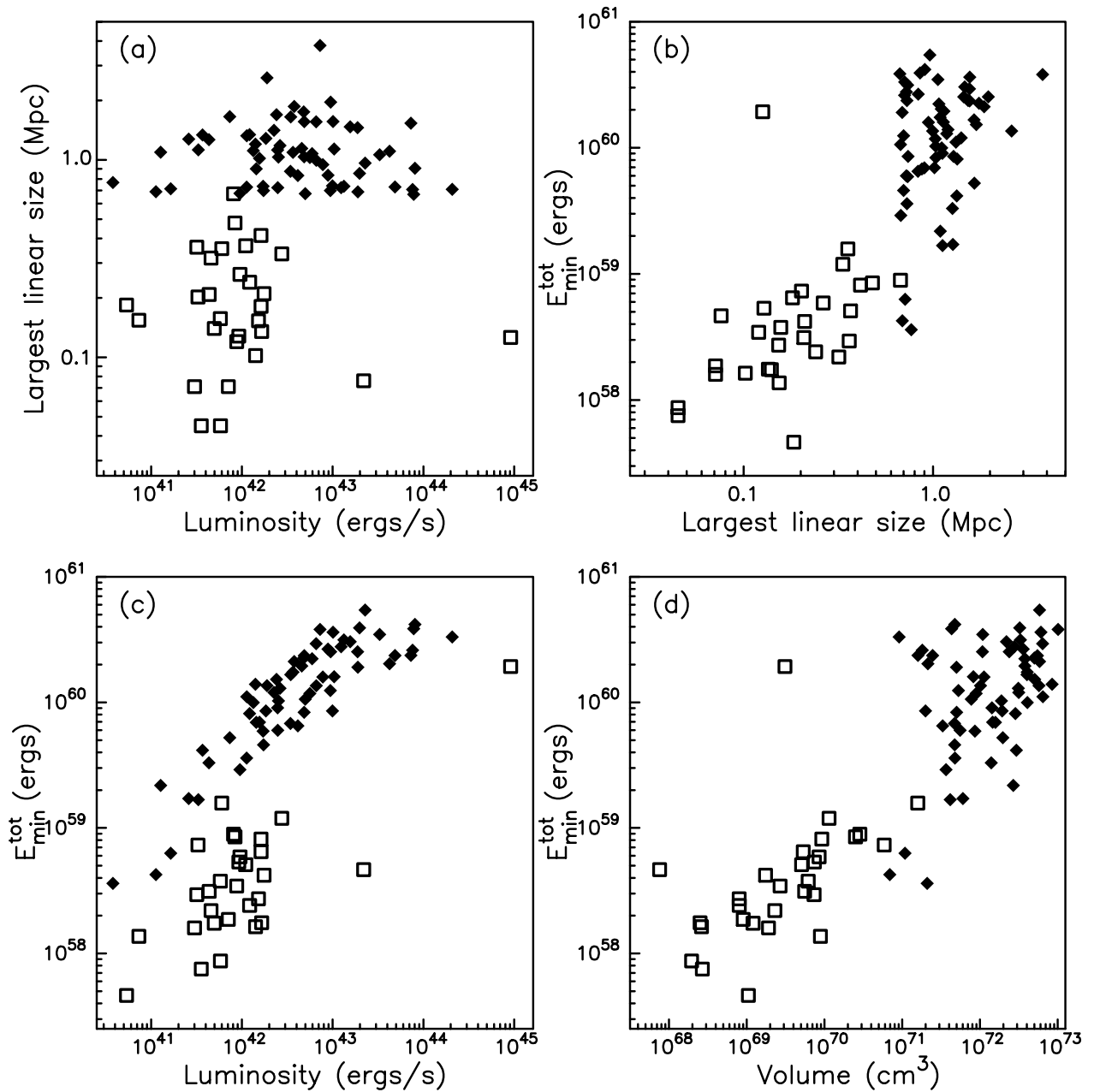


FIG. 1.—Shown are the observed and estimated quantities tabulated in Tables 1 and 2. The giant and cluster sources are represented by solid diamonds and open squares, respectively. Although the groups overlap in their luminosities, their total minimum energies show a marked difference (by a factor of  $\sim 100$ ). A large difference,  $\sim 1000$ , is seen in their estimated volumes as well. Note that three cluster sources, 1222+131, 1246–410, and 1409+52 are not plotted because of their small linear size.

over a large range of source size (e.g., Cotter, Rawlings, & Saunders 1996).

By contrast, when we plot  $E_{\min}^{\text{tot}}$  against LLS or luminosity or volume (Figs. 1b, 1c, and 1d, respectively), a striking separation occurs between sources in these two different environments. The mean energy and volume of cluster sources are smaller by a factor of  $\sim 100$ – $1000$ . Since there is considerable overlap in both luminosity and redshift for these two groups, these striking differences in size and energy (which partially depend on each other) cannot be explained by any luminosity or redshift selection effect. Since we are observing an ensemble of each type of radio source over different evolutionary stages, and since  $E_B$  will gradually build up over time, the *upper envelope* in  $E_{\min}^{\text{tot}}$

(and  $E_B$ ) is significant in the context of this comparison. For example, in a given ICM or IGM environment,  $E_B(t)$  presumably builds up as the source lobes grow in volume, i.e., we would expect some evolutionary migration upwards and to the right in the  $E_{\min}^{\text{tot}}$  versus volume plot in Figure 1d.

It will be important to understand the cause for this large difference in total minimum energy between cluster and giant sources. We can hypothesize that the typical black hole masses of cluster radio galaxies are smaller than those in the giant sources, so that they inherently release less magnetic energy. Alternatively, are AGNs in clusters activated via a different path than those in the typical IGM? Is magnetic field energy dissipated in a different way when the external plasma pressure is different? Unfortunately we do

not understand these systems well enough to completely rule out some of these possibilities.

If, on the other hand, we make the reasonable assumption that the magnetic energy produced by the central black holes is of the same order for both giant and cluster sources, then most ( $\sim 99\%$ ) of the cluster source energy has been lost to the ICM, so that the inferred  $E_{\min}^{\text{tot}}$  of cluster core-embedded sources now is only a tiny residue. Note that the absolute magnitude of this energy is dependent upon various parameters (e.g., the CR proton component) and the minimum energy assumption. The latest generation of cluster X-ray images enable an *independent* energy calculation for the cluster core sources. For at least two sources, Hydra A and Perseus A, the inferred  $PdV$  work done to produce the observed X-ray “holes” that coincide with the radio lobes is

$$E_{pdV} \approx nkT dV \simeq 10^{59} n_{-3} T_8 V_{70} \text{ ergs}, \quad (3)$$

where  $n_{-3}$  denotes normalization to  $10^{-3} \text{ cm}^{-3}$ ,  $T_8$  to  $10^8 \text{ K}$ , and  $V_{70}$  to  $10^{70} \text{ cm}^3$ , which corresponds to a sphere with a radius of 45 kpc. We assume here that the pressure and temperature are constant over this region since the dimensions of the hot gas voids are small compared to the cluster cores. We find that  $E_{pdV}$  is roughly the same as the estimated  $E_{\min}^{\text{tot}}$  of cluster sources. This implies that the magnetic energy output from the central AGNs in clusters is larger than  $E_{pdV}$  by at most a factor of a few. This would still leave their estimated total energy release significantly smaller than the estimated  $E_{\min}^{\text{tot}}$  for giant sources, even with  $k = 0$ , which reduces the giant source energy by approximately a factor of 10 to  $\sim 10^{59} - 10^{60}$  ergs. Furthermore, we might reasonably expect that lobes in the IGM have experienced an equal or larger  $PdV$  work than the ICM sources, due to expansion into a much larger volume (by a factor of  $10^3$ ), even though the thermal pressure of the ICM is higher than the IGM by a factor of  $\sim 10^3 - 10^4$ .

Apart from this unresolved energy difference between giant and cluster sources, they nevertheless have injected an enormous amount of magnetic energy into their environments. We now examine this aspect in more detail.

### 3. THE IMPACT OF MAGNETIC FIELDS

#### 3.1. Magnetic Fields in Intracluster Medium

As discussed in the Introduction, there is now ample evidence that large volumes of the ICM are magnetized, with a total magnetic field energy greater than  $10^{61}$  ergs within the central 500 kpc region of normal rich galaxy clusters (Clarke et al. 2001). It has been argued (Colgate & Li 1999; 2000) that AGNs are responsible for the magnetization of the ICM, motivated by the enormous magnetic flux as well as the large magnetic energy in the ICM. One central point that was emphasized in Colgate & Li (2000) is that black hole accretion disks, besides being responsible for the magnetic energy, may be the most effective magnetic flux multiplier or dynamo in the universe. A total net flux of  $\sim 8 \times 10^4 \mu\text{G kpc}^2$  can be inferred from the characteristic size scale of  $\sim 50 \text{ kpc}$  in, for example, Hydra A (Taylor & Perley 1993; Colgate & Li 2000).

Depending on the typical total magnetic energy released by a single AGN, a total of  $10^{61}/10^{59} - 10^{60} \sim 10 - 100$  AGNs are needed in the lifetime of a cluster in order to fill the cluster with the measured field strength and flux, i.e., it is quite reasonable for AGNs to supply virtually all the mag-

netic energy in a cluster, without the need for other processes such as a turbulent dynamo in the ICM. This is supported by the recently discovered fact that intracluster field strengths out to  $r \sim 500 \text{ kpc}$  are a significant fraction of those found in the inner  $r \leq 100 \text{ kpc}$  core zones (Clarke et al. 2001). This would considerably relax the requirement for magnetic field amplification by turbulence in the inner, high-density zones ( $r \leq 100 \text{ kpc}$ ) of cooling flow clusters. Alternatively stated, if cooling flow-related turbulence is a later stage of ICM evolution, the precooling flow fields are already nearly as strong (Clarke et al. 2001).

Another important effect from these magnetic fields is the heating of the ICM due to magnetic energy dissipation. The addition of a comparable energy component in magnetic fields to the total thermal energy in the ICM could potentially change our understanding of the cluster structure and energetics in a fundamental way.

#### 3.2. Magnetic Fields in the Wider Intergalactic Medium

It has been suggested earlier that the intergalactic medium can be permeated by the magnetic fields from star-driven, magnetized galactic winds at very early epochs, both before  $z \sim 6$  (see Kronberg, Lesch, & Hopp 1999) and since the clusters formed (see Völk & Atoyan 2000). The above discussion has focused on an additional, and potentially more energetic route for the IGM magnetization. Just as AGNs can magnetize the ICM, radio-loud AGNs outside of clusters can be responsible for the magnetic fields in the wider IGM. An interesting question we may ask ourselves is “What happens to those giant radio lobes when the central AGN activities have ceased?” We now examine this question.

To estimate the total magnetic energy generated by radio-loud AGNs, we make the assumption that individual radio-loud QSOs (RLQSOs) will produce roughly similar magnetic energies as radio galaxies, which are the sources studied here. This assumption is supported by the observation that extended RLQSOs have globally similar radio properties to radio galaxies at the same cosmological epoch. The assumption is important because high-redshift RLQSOs may be far more abundant than high-redshift radio galaxies, with the result that their contribution to magnetic fields in the IGM begins with the cosmic epoch at which a significant co-moving density of quasars is built up.

We estimate the mean magnetic energy density from RLQSOs as follows: The present total black hole mass density based on QSOs is

$$\rho_{\text{BH}} \geq 2.2 \times 10^5 / \epsilon_{0.1} M_{\odot} \text{ Mpc}^{-3} \quad (4)$$

where  $\epsilon_{0.1}$  indicates that the efficiency for generating radiation is 0.1 (see Soltan 1982; Chokshi & Turner 1992; Small & Blandford 1992). Depending on the QSO luminosity function evolution, about half of this mass density is already accumulated by  $z \approx 2$  (see Fig. 1 of Chokshi & Turner 1992). If we assume that only 10% of all QSOs are radio-loud (i.e., make powerful radio jets), and that for those RLQSOs about 10% of the black hole accretion energy is converted into magnetic fields, then the mean IGM magnetic field energy density by  $z \approx 2$  is

$$e_B \approx 5 \times 10^{-3} \left( \frac{\epsilon_{\text{RL}}}{0.1} \right) \left( \frac{\epsilon_B}{0.1} \right) \rho_{\text{BH}} \approx 7.3 \times 10^{-17} \text{ ergs cm}^{-3}, \quad (5)$$

where  $\epsilon_{\text{RL}}$  and  $\epsilon_B$  stand for the ratio of RLQSOs to all QSOs and the efficiency for them making magnetic fields, respectively. This energy density is comparable to the thermal pressure of the IGM at  $z \approx 2$ ,

$$p_{\text{IGM}} \approx 1.6 \times 10^{-16} \left( \frac{n-4}{10^{-4}} \right) \left( \frac{T_4}{10^4} \right) \text{ ergs cm}^{-3}. \quad (6)$$

In other words, if all the magnetic field energy were spread out throughout the whole universe, the IGM would be a  $\beta = p_{\text{IGM}}/e_B \approx 2$  plasma, with a comparable thermal and magnetic pressure.

The actual impact of these magnetic fields on the IGM will be determined by whether these magnetic fields can indeed fill up the whole (or a significant fraction of the) volume of the IGM. Note that the visible magnetized lobes are created in a very short time ( $\sim 10^7$ – $10^8$  yr) compared to the age of the universe. Since they could be overpressured relative to the surrounding medium by a large factor (at least  $\sim 100$ ), further expansion seems inevitable. Estimates by Furlanetto & Loeb (2001) suggest that the magnetic fields from QSOs can fill up 5%–20% of the IGM volume, comparable to Kronberg et al.'s (1999) estimate of the starburst-driven IGM filling that is most effective at  $z \geq 7$ . Since magnetic fields made by AGNs are likely to be highly structured, we expect that their expansion might be quite different from the usual adiabatic expansion. However, detailed calculations are needed to show this.

The physics of this expansion holds the key to a *quantitative* understanding of the impact of magnetic fields on the dynamics of the IGM. Since the QSO activity peaks around  $z \sim 2$ – $3$ , the subsequent baryonic dynamics, and the formation of galaxies and of large-scale structure approaching galaxy scales are likely to be modified significantly by these magnetic fields.

A highly magnetized IGM appears tentatively consistent with the discovery of diffuse, 326 MHz synchrotron emission well beyond the boundaries of the Coma Cluster of galaxies by Kim et al. (1989). The low-level synchrotron “glow” that they found extending beyond the Coma Cluster gave supracluster intergalactic  $B_{\text{minE}}$  values between  $10^{-7}$  and  $10^{-6}$  G over linear dimensions a few times the core size of the Coma cluster itself. A consequence of our suggestion that the IGM is directly energized by AGN-generated magnetic flux is that more widespread synchrotron glow will be seen over larger IGM volumes, which can be tested in future when more sensitive low frequency radio images are available.

#### 4. CONCLUSIONS

We have analyzed the minimum energy content of the radio lobes of  $\sim 100$  powerful radio galaxies,  $\sim 70$  of which

reside in a typical low-density IGM and  $\sim 30$  within the inner cores of rich galaxy clusters. These two groups show a large difference in the estimated total magnetic energy, with cluster sources having  $\sim 10^{58}$ – $10^{59}$  ergs whereas giant sources have  $\sim 10^{60}$ – $10^{61}$  ergs. The latter is a significant fraction of the total energy released from the formation of a typical  $10^8 M_\odot$  black hole.

We emphasize that the observed magnetic energy underestimates that made by the black hole accretion, due to various losses incurred while magnetic fields expand to form the giant radio lobes. This is especially true for cluster sources where we find that a comparable or perhaps even larger amount of energy is expended as  $PdV$  work in displacing the hot, dense ICM gas surrounding the lobes.

The storing of large amounts of energy in magnetic fields is a unique way for AGNs to impact their surrounding medium. The AGN energy released via radiation loses its dynamic impact when the medium becomes optically thin. By contrast, the AGN energy released via magnetic fields can maintain its *dynamical* impact over the age of the universe, because most of this energy is contained in a large volume around the galaxy. This fact may have important consequences for galaxy and structure evolution.

From our estimated magnetic energies arising from radio galaxies in clusters, we argue that these AGNs can be solely responsible for the large magnetic energy and flux, i.e., the magnetization of the whole ICM, as revealed by recent radio and X-ray observations. The magnetic fields from these AGNs may also provide an important heating source for the whole ICM.

We further suggest that the total magnetic energy from radio-loud QSOs/AGNs is *energetically* important, especially at the epoch of  $z \sim 2$ – $3$  when QSO activity peaks. Giant lobes from each “magnetic” AGN are usually highly overpressured compared to the typical IGM, thus further expansion of these lobes (after the central AGN activity has ceased) is likely to provide the space-volume filling process that could magnetize the whole (or a significant fraction of the) IGM. Detailed calculations of such processes will be presented in future publications.

We acknowledge useful conversations with T. Able, R. Daly, and M. Norman at an Aspen winter workshop on Galaxy Formation. P. P. K. and Q. W. D. acknowledge support from an NSERC of Canada grant A5713, and P. P. K. is grateful for support from the Canada Council's Killam Program. The research of H. L. and S. A. C. is performed under the auspices of the US Department of Energy and is supported in part by an IGPP/Los Alamos grant and the Laboratory Directed Research and Development Program at Los Alamos.

#### REFERENCES

- Alexander, P., & Leahy, J. P. 1987, MNRAS, 225, 1  
 Andernach, H., Baker, J. R., von Kap-Herr, A., & Wielebinski, R. 1979, A&A, 74, 93  
 Baars, J. W. M., Genzel, R., Pauliny-Toth, I. I. K., & Witzel, A. 1977, A&A, 61, 99  
 Begelman, M. C., Blanford, R. D., & Rees, M. J. 1984, Rev. Mod. Phys, 56, 255  
 Bhatnagar, S., Gopal-Krishna, & Wisotzki, L. 1998, MNRAS, 299, L25  
 Bridle, A. H., & Perley, R. A. 1984, ARA&A, 357, 373  
 Burbidge, G. R. 1956, ApJ, 124, 416  
 ———. 1958, ApJ, 129, 849  
 Burbidge, G. R., & Burbidge, E. M. 1965, in The Structure and Evolution of Galaxies, Proc. 13th (Solvay) Conf. on Physics, Bruxelles (New York: Interscience), 137  
 Carilli, C. L., Perley, R. A., Dreher, J. W., & Leahy, J. P. 1991, ApJ, 383, 554  
 Chokshi, A., & Turner, E. L. 1992, MNRAS, 259, 421  
 Clarke, T. E., Kronberg, P. P., & Böhringer, H. 2001, ApJ, 547, L111  
 Colgate, S. A., & Li, H. 1999, Ap&SS, 264, 357  
 ———. 2000, in IAU Symp. 195, Highly Energetic Physical Processes and Mechanisms for Emission from Astrophysical Plasmas, ed. P. C. H. Martens, S. Tsurta, & M. A. Weber (ASP: San Francisco), 255  
 Colgate, S. A., Li, H., & Pariev, V. 2001, Physics of Plasmas, in press  
 Condon, J. J., Cotton, W. D., Greisen, E. W., Yin, Q. F., Perley, R. A., Taylor, G. B., & Broderick, J. J. 1998, AJ, 115, 1693  
 Cotter, G., Rawlings, S., & Saunders, R. 1996, MNRAS, 281, 1081  
 Dallacasa, D., Feretti, L., Giovannini, G., & Venturi, T. 1989, A&AS, 79, 391  
 Danziger, I. J., Goss, W. M., & Frater, R. H. 1978, MNRAS, 184, 341



- de Bruyn, A. G. 1989, *A&A*, 226, L13
- Eilek, J. A. 1999, in *Diffuse Thermal and Relativistic Plasma in Galaxy Clusters*, ed. H. Böhringer, L. Feretti & P. Schuecker, MPE Rep. 271
- Eilek, J. A., Burns, J. O., O'Dea, C. P., & Owen, F. N. 1984, *ApJ*, 278, 37
- Ekers, R. D., Fanti, R., Lari, C., & Parma, P. 1981, *A&A*, 101, 194
- Ekers, R. D., Goss, W. M., Wellington, K. J., Bosma, A., Smith, R. M., & Schweizer, F. 1983, *A&A*, 127, 361
- Fabian, A. C., et al. 2000, *MNRAS*, 318, 65L
- Feretti, L., Dallacasa, D., Giovannini, G., & Tagliani, A. 1995, *A&A*, 302, 680
- Feretti, L., Dallacasa, D., Govoni, F., Giovannini, G., Taylor, G. B., & Klein, U. 1999, *A&A*, 344, 472
- Furlanetto, S. R., & Loeb, A. 2001, *ApJ*, 556, 619
- Gregorini, L., Padrielli, L., Parma, P., & Gilmore, G. 1988, *A&AS*, 74, 107
- Hargrave, P. J., & Ryle, M. 1974, *MNRAS*, 166, 305
- Herbig, T., & Readhead, A. C. S. 1992, *ApJS*, 81, 83
- Hine, R. G. 1979, *MNRAS*, 189, 527
- Hines, D. C., Eilek, J. A., & Owen, F. N. 1989, *ApJ*, 347, 713
- Hoyle, F., Fowler, W. A., Burbidge, G. R., & Burbidge E. M. 1964, *ApJ*, 139, 909
- Ishwara-Chandra, C. H., & Saikia, D. J. 1999, *MNRAS*, 309, 100
- Jägers, W. J. 1987a, *A&AS*, 71, 75
- . 1987b, *A&AS*, 67, 395
- Jägers, W. J., Miley, G. K., van Breugel, W. J. M., Schilizzi, R. T., & Conway, R. G. 1982, *A&A*, 105, 278
- Jones, P. A. 1986, *Proc. Astron. Soc. Australia*, 6, 329
- Jones, P. A., & McAdam, W. B. 1992, *ApJS*, 80, 137
- Kapahi, V. K., Athreya, R. M., van Breugel, W., McCarthy, P. J., & Subrahmanya, C. R. 1998, *ApJS*, 118, 275
- Kassim, N. E., Perley, R. A., Erickson, W. C., & Dwarakanath, K. S. 1993, *AJ*, 106, 2218
- Kim, K. T., Kronberg, P. P., Dewdney, P. E., & Landecker, T. L. 1990, *ApJ*, 255, 29
- Kim, K. T., Kronberg, P. P., Giovannini, G., & Venturi, T. L. 1989, *Nature*, 341, 720
- Kronberg, P. P. 1994, *Prog. Phys.*, 57, 325
- Kronberg, P. P., Lesch, H., & Hopp, U. 1999, *ApJ*, 511, 56
- Kronberg, P. P., Wielebinski, R., & Graham, D. A. 1986, *A&A*, 169, 63
- Lacy, M., Rawlings, S., Saunders, R., & Warner, P. J. 1993, *MNRAS*, 264, 721
- Laing, R. A., & Bridle, A. H. 1987, *MNRAS*, 228, 557
- Lara, L., Mack, K.-H., Lacy, M., Klein, U., Cotton, W. D., Feretti, L., Giovannini, G., & Murgia, M. 2000, *A&A*, 356, 63
- Lara, L., Márquez, I., Cotton, W. D., Feretti, L., Giovannini, G., Marcaide, J. M., & Venturi, T. 1999, *A&A*, 348, 699
- Leahy, J. P., & Perley, R. A. 1991, *AJ*, 102, 537
- Leahy, J. P., Pooley, G. G., & Riley, J. M. 1986, *MNRAS*, 222, 753
- Machalski, J., & Condon, J. J. 1985, *AJ*, 90, 5
- Mack, K.-H., Klein, U., O'Dea, C. P., & Willis, A. G. 1997, *A&AS*, 123, 423
- Masson, C. R. 1979, *MNRAS*, 187, 253
- Mayer, C. J. 1979, *MNRAS*, 186, 99
- McNamara, B. R., et al. 2000, *ApJ*, 534, L135
- Nilsson, K. 1997, Ph.D thesis, Univ. Turku, Finland
- Owen, F. N., & Ledlow, M. J. 1997, *ApJS*, 108, 41
- Owen, F. N., O'Dea, C. P., Inoue, M., & Eilek, J. A. 1985, *ApJ*, 294, L85
- O'Dea, C. P., & Owen, F. N. 1985, *AJ*, 90, 927
- O'Donoghue, A. A., Eilek, J. A., & Owen, F. N. 1990, *ApJS*, 72, 75
- Pacholczyk, A. G. 1970, *Radio Astrophysics* (San Francisco: Freeman)
- Palma, C., Bauer, F. E., Cotton, W. D., Bridle, A. H., Majewski, S. R., & Sarazin, C. L. 2000, *AJ*, 119, 2068
- Parma, P., de Ruiter, H. R., Mack, K.-H., van Breugel, W., Dey, A., Fanti, R., & Klein, U. 1996, *A&A*, 311, 49
- Pedlar, A., Ghataure, H. S., Davies, R. D., Harrison, B. A., Perley, R., Crane, P. C., & Unger, S. W. 1990, *MNRAS*, 246, 477
- Perley, R. A., & Taylor, G. B. 1991, *AJ*, 101, 1623
- Riley, J. M., Warner, P. J., Rawlings, S., Saunders, R., Pooley, G. G., & Eales, S. A. 1989, *MNRAS*, 236, 13
- Röttgering, H. J. A., Tang, Y., Bremer, M. A. R., de Bruyn, A. G., Miley, G. K., Rengelink, R. B., & Bremer, M. N. 1996, *MNRAS*, 282, 1033
- Rottmann, H., Mack, K.-H., Klein, U., & Wielebinski, L. 1996, *A&A*, 309, 19
- Saripalli, L., Gopal-Krishna, Reich, W., & Kühr, H. 1986, *A&A*, 170, 20
- Saripalli, L., Mack, K.-H., Klein, U., Strom, R., & Singal, A. K. 1996, *A&A*, 306, 708
- Saripalli, L., Subrahmanyan, R., & Hunstead, R. W. 1994, *MNRAS*, 269, 37
- Saunders, R., Baldwin, J. E., & Warner, P. J. 1987, *MNRAS*, 225, 713
- Schoenmakers, A. P., de Bruyn, A. G., Röttgering, H. J. A., & van der Laan, H. 1999, *A&A*, 341, 44
- . 2000a, *MNRAS*, 315, 395
- Schoenmakers, A. P., Mack, K.-H., de Bruyn, A. G., Röttgering, H. J. A., Klein, U., & van der Laan, H. 2000b, *A&AS*, 146, 293
- Schoenmakers, A. P., Mack, K.-H., Lara, L., Röttgering, H. J. A., de Bruyn, A. G., van der Laan, H., & Giovannini, G. 1998, *A&A*, 336, 455
- Small, T. A., & Blandford, R. D. 1992, *MNRAS*, 259, 725
- Snellen, I. A. G., Zhang, M., Schilizzi, R. T., Röttgering, H. J. A., de Bruyn, A. G., & Miley, G. K. 1995, *A&A*, 300, 359
- Soltan, A. 1982, *MNRAS*, 200, 115
- Strom, R. G., Baker, J. R., & Willis, A. G. 1981, *A&A*, 100, 220
- Strom, R. G., Riley, J. M., Spinrad, H., van Breugel, W. J. M., Djorgovski, S., Liebert, J., & McCarthy, P. J. 1990, *A&A*, 227, 19
- Subrahmanya, C. R., & Hunstead, R. W. 1986, *A&A*, 170, 27
- Subrahmanyan, R., Saripalli, L., & Hunstead, R. W. 1996, *MNRAS*, 279, 257
- Taylor, G. B., Allen, S. A., & Fabian, A. C. 1999, in *Diffuse Thermal and Relativistic Plasma in Galaxy Clusters*, ed. H. Böhringer, L. Feretti & P. Schuecker, MPE Rep. 271
- Taylor, G. B., & Perley, R. A. 1993, *ApJ*, 416, 554
- Taylor, G. B., Perley, R. A., Inoue, M., Kato, T., Tabara, H., & Aizu, K. 1990, *ApJ*, 360, 41
- Turland, B. D. 1975, *MNRAS*, 170, 281
- van Breugel, W. J. M., & Willis, A. G. 1981, *A&A*, 96, 332
- Vigotti, M., Grueff, G., Perley, R., Clark, B. G., & Bridle, A. H. 1989, *AJ*, 98, 419
- Völk, H. J., & Atoyan, A. M. 2000, *ApJ*, 541, 88
- Wan, L., Daly, R. A., & Guerra, E. J. 2000, *ApJ*, 544, 671
- Willis, A. G., & Strom, R. G. 1978, *A&A*, 62, 375
- Willis, A. G., Strom, R. G., Perley, R. A., & Bridle, A. H. 1982, in *IAU Symp. 97, Extragalactic Radio Sources*, ed. D. S. Heeschen & C. M. Wade (Dordrecht: Reidel), 141
- Wilson, A. S., Young, A. J., & Shopbell, P. L. 2001, *ApJ*, 547, 740
- Zukowski, E. L. H. 1990, Ph.D thesis, Univ. Toronto, Toronto